

# Resonant-Boost-Input Three-Phase Power Factor Corrector

Da Feng Weng, *Member, IEEE* and S. Yuvarajan, *Senior Member, IEEE*

**Abstract**—This paper presents a novel three-phase power factor corrector (PFC) circuit which uses two power switches working in zero-voltage-switching (ZVS) condition. The two switches along with a high-frequency inductor constitute a high-frequency current source which is responsible for the energy transfer in the circuit. The input current is partly continuous and partly discontinuous. The total harmonic distortion (THD) in the input current has a low value of 4.5%, and the output dc voltage is very close to the peak line voltage. The operation of the converter is explained by identifying the different switching modes, and the simulation and experimental waveforms are presented.

**Index Terms**—Boost topology, three-phase ac-dc power conversion, zero-voltage switching.

## I. INTRODUCTION

THREE-PHASE converters are used to handle large powers while maintaining a balanced operation of the ac mains. Several power factor corrector (PFC) topologies and control methods for reducing the input current harmonics have been presented in recent years. Due to the higher efficiency of the topology, the boost-type PFC is being considered for several applications. Based on the input current of the converter, the operation could be in the continuous current mode (CCM) or in the discontinuous current mode (DCM).

A three-phase PFC converter operating in the CCM [1] is composed of six power switches, six ultrafast diodes, and three inductors as shown in Fig. 1. Current control loops are used to shape the input current waveform. Since each input phase-current is shaped by a separate current loop, the output voltage of the converter can be made to follow the peak line-line voltage resulting in a low value of total harmonic distortion (THD) in the input current. Since the current is continuous, the switches in the converter will be subjected to hard-switching condition unless some soft-switching circuits are added. Wide-band current sensors are required to detect each of the input current in order to implement the current loop. Due to the continuous nature of the current in the loop, a complex compensation circuit will be needed to ensure system stability. The nature of the control is such that the current loop essentially controls the equivalent duty cycle of the input

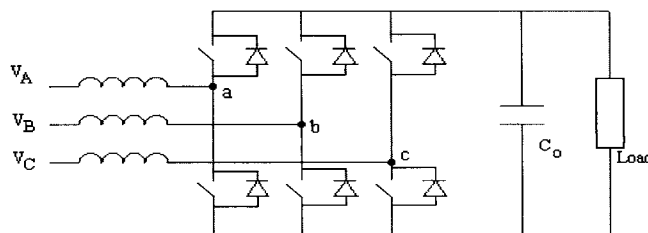


Fig. 1. Power circuit of three-phase PFC of [1].

inductor. This is done by controlling the duty cycle of the power switches.

A three-phase PFC converter with DCM [2] is composed of one power switch, three boost inductors, three differential chokes, and seven ultrafast diodes as shown in Fig. 2. The input currents are partly shaped by the power switch. The decay time of the boost-inductor current during a switching cycle is determined by the difference between the output dc voltage and the input voltage during that cycle. The decaying portions of the current are not controlled by the power switch. One way to reduce these decay currents is to increase the difference between the output voltage and the amplitude of the input voltage. The other method is to control the equivalent duty cycle of the input inductor which is almost the same as the one used in the continuous current case. In a single-phase PFC, second-harmonic injection is used to control the equivalent duty cycle of the input inductor [3]. In this way, the input current is shaped and the THD in the input current is reduced. In the control scheme, the equivalent duty cycle is controlled by controlling the duty cycle of the power switch. For a three-phase system, the use of some modulation techniques in controlling the equivalent duty cycle of each phase current has been described [4]. Due to the coupling present in the three-phase system, it is difficult to decrease the THD drastically [5]. In order to keep the THD value low, generally, the converter will be designed with a higher output voltage which is not good for the succeeding converter in a cascade. It is clear that the only way to reduce the THD in a three-phase system is to decouple and control each phase separately.

From the control system point of view, a three-phase PFC operating in CCM can be decoupled into three single-phase systems (converters). Each system is independently controlled by a separate current loop in order to keep a low THD and a low output voltage. In a three-phase PFC with a discontinuous current, however, only one switch is used to control all the three input currents. Thus, it is not possible to split or decouple

Manuscript received March 13, 1998; revised April 23, 1998. Recommended by Associate Editor, M. Elbuluk.

D. F. Weng is with Matsushita Electric Works (R&D), Woburn, MA 01801 USA.

S. Yuvarajan is with the Department of Electrical Engineering, North Dakota State University, Fargo, ND 58105 USA.

Publisher Item Identifier S 0885-8993(99)08899-7.

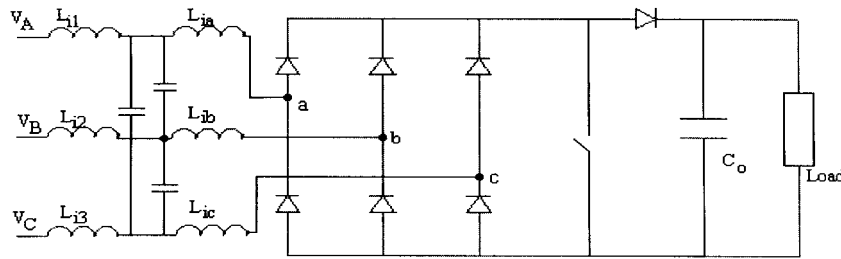


Fig. 2. Power circuit of three-phase PFC of [2].

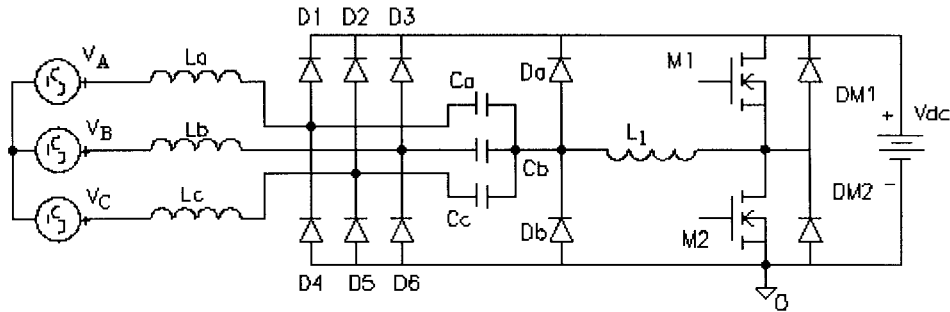


Fig. 3. Power circuit of the proposed three-phase PFC converter.

the three-phase system into three single-phase systems and to control each phase independently. A single-phase PFC in which the input current is discontinuous over the lower range of instantaneous ac line voltage and continuous over the higher instantaneous voltage range has been presented as a hybrid between the CCM and DCM [6].

A new topology for a resonant boost input (RBI) three-phase PFC converter is presented in this paper. In this topology, three capacitors are used to decouple the three-phase system into three single-phase systems and to control each phase independently. It is the independent control of each single-phase system that helps to obtain a low THD value for each input current even for a low-output dc voltage. Comparing the converters of [1] (Fig. 1) and [2] (Fig. 2), the proposed circuit is simple and the cost will be low. All the power switches will be turned on or off under zero-voltage-switching (ZVS) condition. The circuit is ideally suitable for operation at high switching frequencies which will reduce the size of the converter.

II. STRUCTURE AND PRINCIPLE OF OPERATION

The power circuit of the proposed converter is shown in Fig. 3. The circuit is composed of three differential chokes, six ultrafast diodes, one high-frequency inductor (\$L\_1\$), two general-purpose diodes, three input capacitors, and two power switches. In the circuit, \$D\_a\$, \$D\_b\$, \$M\_1\$, \$M\_2\$, and \$L\_1\$ constitute a high-frequency current source. The current source discharges the capacitors \$C\_a\$, \$C\_b\$, and \$C\_c\$, and transfers the energy stored in \$C\_a\$, \$C\_b\$, and \$C\_c\$ to the dc filter capacitor \$C\_{dc}\$ (here, the value of the capacitor is very high, and it is replaced by a dc voltage source \$V\_{dc}\$).

For a balanced three-phase system, the converter can be decoupled into three single-phase PFC converters (Fig. 4), each of which is a single-phase doubler PFC converter. The

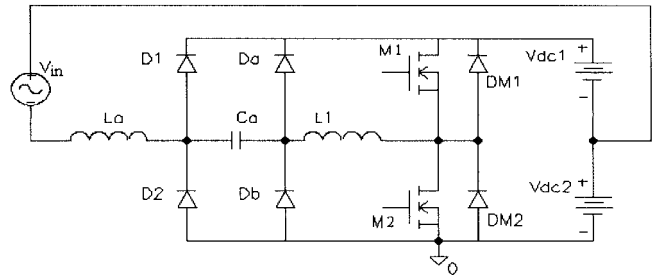


Fig. 4. Power circuit of equivalent single-phase PFC converter.

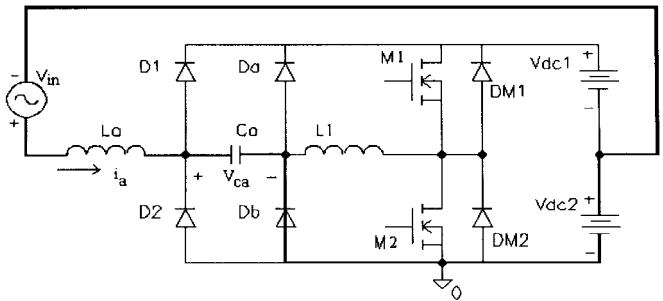


Fig. 5. (a) Equivalent circuit during Mode 1 and (b) the waveform of input current.

input capacitor \$C\_a\$ transfers part of the input energy to the inductor \$L\_1\$ and the energy is then transferred to the dc filter capacitor and the load. Depending on the magnitude of the

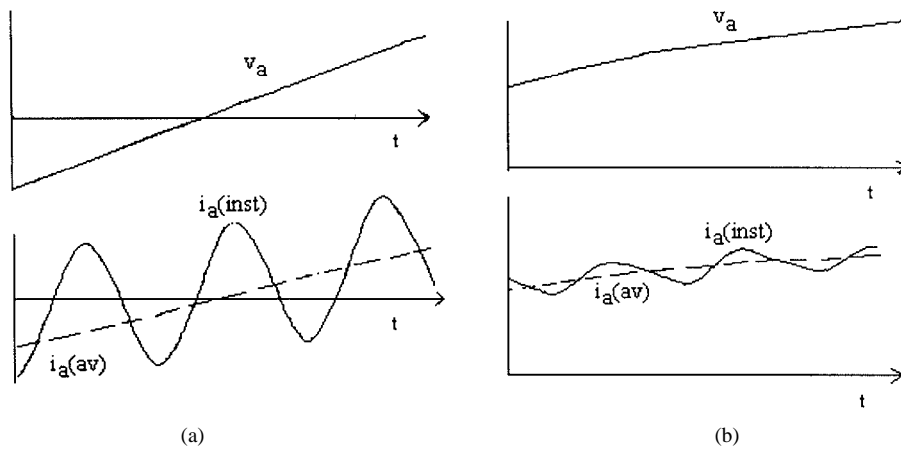


Fig. 6. Illustrative waveforms of  $v_a$ ,  $i_a$  (instantaneous), and  $i_a$  (average) for (a) discontinuous input current and (b) continuous input current.

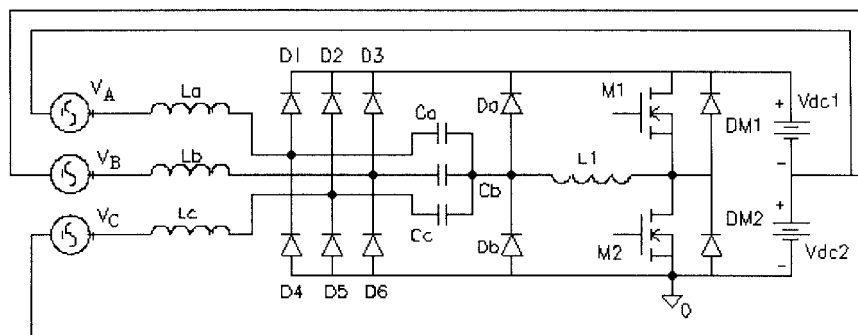


Fig. 7. Combination of the three single-phase doubler PFC converters.

instantaneous input voltage, the circuit may operate under: 1) a resonant input mode or 2) a boost input mode. The resonant input mode corresponds to a low instantaneous input voltage, and during this mode, the voltage on  $C_a$  is always less than  $(V_{dc1} + V_{dc2})$ . The boost input mode, on the other hand, corresponds to a high instantaneous input voltage, and during this mode the voltage on  $C_a$  approaches  $(V_{dc1} + V_{dc2})$ .

The resonant input mode can be further divided into six switching modes. In the analysis, only the positive half cycle of the input voltage is considered. The operation during the negative half cycle can be analyzed in the same way.

**Mode 1:** The switch  $M_2$  is turned on. Assuming the current in  $L_1$  to be larger than the current in the differential choke  $L_a$ , the diode  $D_b$  turns on. The input capacitor  $C_a$  is charged by  $V_1(V_{in})$  through  $L_a$ . The voltage across  $C_a$  increases, but it will be less than  $(V_{dc1} + V_{dc2})$ .

**Mode 2:** Once the switch  $M_2$  is turned off, the current through  $L_1$  continues through  $DM1$  and switch  $M_1$  is turned on under ZVS condition. The energy stored in  $L_1$  is released to the dc capacitor  $(V_{dc1} + V_{dc2})$  through  $D_b$  and  $DM1$ . The current in  $L_1$  will decrease to zero causing  $D_b$  to turn off.

**Mode 3:** The capacitor  $C_a$  with its initial voltage resonates with  $L_1$  and the resonant current flows through  $D_1$  and  $M_1$ . The energy stored in  $C_a$  is transferred to  $L_1$  and the energy stored in  $L_a$  is released to  $V_{dc1}$  through  $D_1$ .

**Mode 4:** As the voltage on  $C_a$  drops below zero,  $D_a$  is turned on. The voltage on  $C_a$  is clamped to zero and there

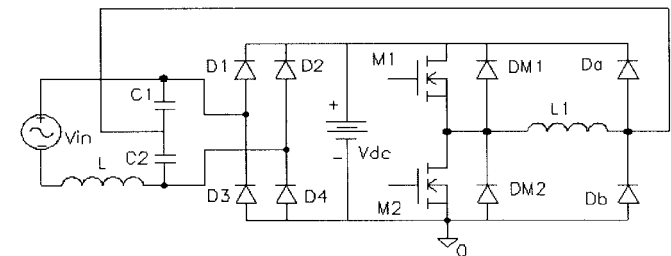


Fig. 8. Combination of two single-phase doubler PFC converters.

is a circulating current flowing through  $D_a$ ,  $L_1$ , and  $M_1$ . The energy stored in  $L_a$  continues to be released to  $V_{dc1}$  through  $D_1$ .

**Mode 5:** As the switch  $M_1$  turns off, the switch  $M_2$  can be turned on under ZVS condition. The energy stored in  $L_1$  will be released to  $(V_{dc1} + V_{dc2})$  through  $D_a$  and  $DM2$ . The current in  $L_1$  will decrease to zero, and then  $D_a$  is turned off. The energy stored in  $L_a$  continues to be released to  $V_{dc1}$  through  $D_1$ .

**Mode 6:** The switch  $M_2$  is turned on. The capacitor  $C_a$  will resonate with  $L_1$  and the current through  $L_1$  increases. As the current through  $L_1$  exceeds the input current,  $D_1$  will be turned off and  $D_b$  will turn on and carry the current of  $L_1$ . The switching process will go back to Mode 1.

The boost input mode can be divided into the following seven switching modes.

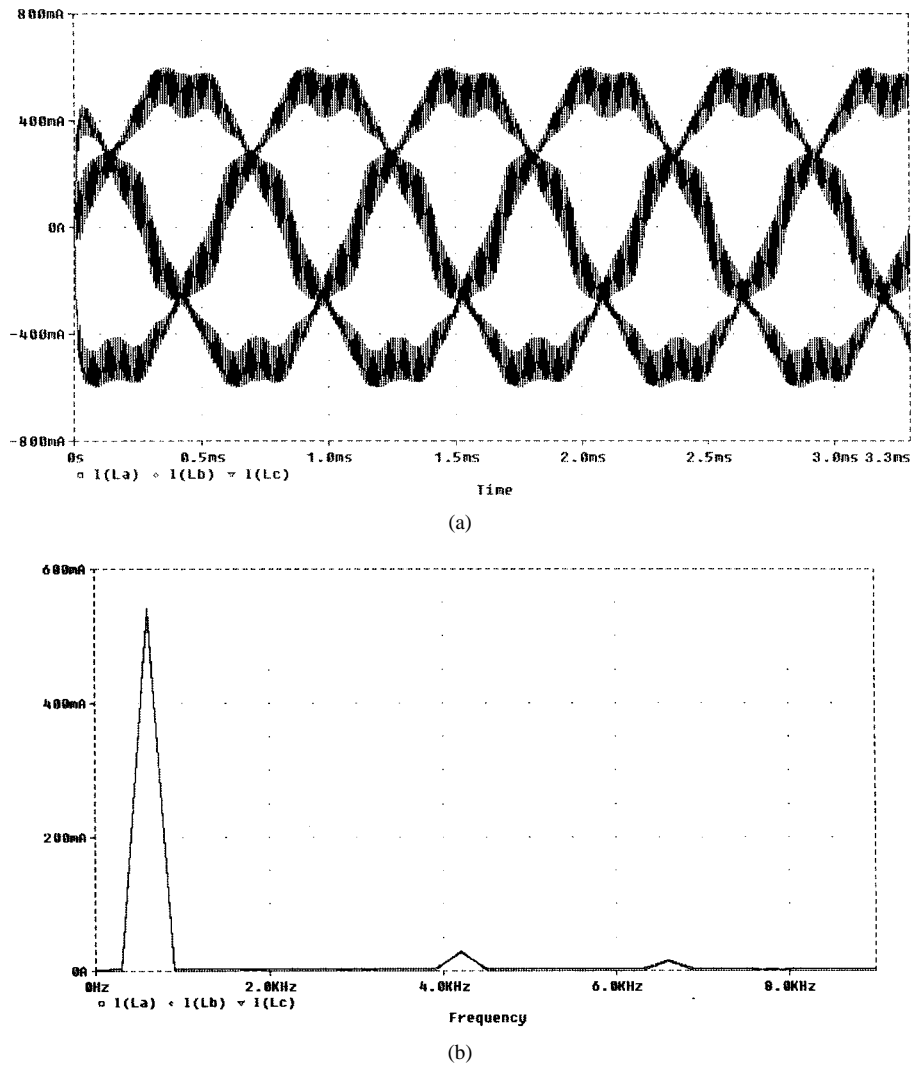


Fig. 9. (a) Simulation waveforms of the input currents. (b) Frequency spectra of the waveforms of Fig. 9(a).

*Mode 1:* The switch  $M_2$  is turned on. The input capacitor  $C_a$  is charged by  $V_{in}$  through  $L_a$ . The voltage on  $C_a$  increases until it reaches  $(V_{dc1} + V_{dc2})$ .

*Mode 2:* Once the voltage on  $C_a$  exceeds  $(V_{dc1} + V_{dc2})$ ,  $D_1$  will be turned on and the energy stored in  $L_a$  will be released to  $V_{dc1}$ . A circulating current flows through  $D_b$ ,  $L_1$ , and  $M_2$ .

*Mode 3:* The switch  $M_2$  is turned off and switch  $M_1$  is turned on under ZVS condition. The energy stored in  $L_1$  is released to the dc bulk capacitor  $(V_{dc1} + V_{dc2})$ . As a result, the current in  $L_1$  will decrease to zero. It will cause  $D_b$  to turn off. The inductor  $L_a$  will continue releasing the stored energy to  $V_{dc1}$  through  $D_1$ .

*Mode 4:* The capacitor  $C_a$  with its initial voltage will resonate with  $L_1$  and the resonant current flows through  $D_1$  and  $M_1$ . The energy stored in  $C_a$  is transferred to  $L_1$  and the energy stored in  $L_a$  continues to be released to  $V_{dc1}$  through  $D_1$ .

*Mode 5:* As the voltage across  $C_a$  drops below zero,  $D_a$  is turned on. The voltage on  $C_a$  is clamped to zero and a circulating current flows through  $D_a$ ,  $L_1$ , and  $M_1$ . The energy stored in  $L_a$  continues to be released to  $V_{dc1}$  through  $D_1$ .

*Mode 6:* As the switch  $M_1$  turns off, the switch  $M_2$  can be turned on under ZVS condition. The energy stored in  $L_1$  will be released to  $(V_{dc1} + V_{dc2})$  through  $D_a$  and  $D_{M2}$ . The current in  $L_1$  will decrease to zero, and then  $D_a$  is turned off. The energy stored in  $L_a$  continues to be released to  $V_{dc1}$  through  $D_1$ .

*Mode 7:* The switch  $M_2$  is turned on. The capacitor  $C_a$  will resonate with  $L_1$  and the current in  $L_1$  increases. As the current in  $L_1$  exceeds the input current in  $L_a$ ,  $D_1$  will be turned off and  $D_b$  will turn on and carry the current in  $L_1$ . The switching process will then be back to Mode 1.

From the operation of the circuit, it is clear that, because of input capacitor  $C_a$ , the input voltage modulates the equivalent duty cycle of the single phase converter, and the circuit automatically shapes the input current. During the resonant-input mode 1 and the boost-input mode 1, the instantaneous input voltage charges the input capacitor  $C_a$  through the input inductor  $L_a$  as shown in Fig. 5. The volt-second VDT exciting the input inductor  $L_a$  is given by

$$VDT = \int_0^{t_f} V_L(t) \cdot dt = C_a \cdot R_{equ} \cdot \frac{[V_{in} + V_{dc2} - V_{ca}(0)]^2}{2 \cdot V_{in}} \quad (1)$$

where  $V_L$  is the voltage across  $L_a$ ,  $t_f$  is time during which the inductor voltage is positive,  $R_{\text{equ}}$  is the equivalent resistance of the converter,  $V_{\text{in}}$  is the instantaneous ac input voltage, and  $V_{ca}(0)$  is value of the capacitor voltage when the inductor current starts increasing. The expression for the excitation volt-second on the input inductor shows that the value of VDT changes with the instantaneous input voltage, that is, for a low value of instantaneous voltage, the volt-second VDT is high and vice versa. The equivalent duty cycle  $D_{\text{equ}} (= t_f/T)$  of the input inductor can be obtained from (1) as

$$D_{\text{equ}} = C_a \cdot R_{\text{equ}} \cdot f_s \cdot \frac{[V_{\text{in}} + V_{\text{dc}2} - V_{ca}(0)]^2}{2 \cdot V_{\text{in}} \cdot (V_{\text{in}} + V_{\text{dc}2})} \quad (2)$$

where  $f_s = 1/T$  is the switching frequency. If  $V_{ca}(0)$  is much smaller than  $V_{\text{in}} + V_{\text{dc}2}$ ,  $D_{\text{equ}}$  can be approximated as

$$D_{\text{equ}} \approx C_a \cdot R_{\text{equ}} \cdot f_s \cdot \frac{(V_{\text{in}} + V_{\text{dc}2})}{2 \cdot V_{\text{in}}} \quad (3)$$

Equation (3) shows that the equivalent duty cycle  $D_{\text{equ}}$  varies with the input line voltage. If the instantaneous input voltage is low, the equivalent duty cycle is high and vice versa. The illustrative waveforms of  $v_a$ ,  $i_a$  (instantaneous), and  $i_a$  (average) for the discontinuous and continuous cases are shown in Fig. 6. The input current is discontinuous for low instantaneous input voltages. Since there are no diodes, the current goes from positive maximum to a negative minimum.

The form of equivalent duty-cycle variation is the same as one required in the CCM control and the DCM-modulated control. In the volt-second calculation, the duty cycle of the power switch is not considered. The duty cycle of the power switch can be almost independent of the volt-second control. The duty cycle of the power switch (turn on or off) is just used to provide a high-frequency current source to discharge the energy stored in the input capacitor  $C_a$  and transfer the energy to the dc filter capacitor ( $V_{\text{dc}1} + V_{\text{dc}2}$ ). The input inductor exciting time  $D_{\text{eq}}T$  is equal to the time interval during which the input capacitor  $C_a$  is charged from the initial voltage to the dc bulk voltage. If the dc bulk voltage is low, the exciting time will be low and the volt-second on the input inductor will be low. Thus, it is possible to choose the output dc voltage very close the input voltage amplitude. In other words, the rectifier voltage gain  $M = V_{\text{dc}}/V_{U,m}$  can be chosen to be closer to one.

During each switching period, the input capacitor is charged by the instantaneous input voltage  $V_{\text{in}}$  through the input inductor and discharged by the high-frequency current source. The amplitude of the high-frequency current source will affect the initial voltage on the input capacitor  $C_a$ . The higher the amplitude of the high-frequency current source, the lower the initial voltage on the input capacitor  $C_a$  will be. From (1) to (3), it is clear that the exciting time of the input inductor  $L_a$  is determined by the difference between the initial voltage of  $C_a$ ,  $V_{ca}(0)$ , and the final voltage of  $C_a$ , which is equal to the dc bulk voltage ( $V_{\text{dc}1} + V_{\text{dc}2}$ ) and the instantaneous input current. The higher the voltage difference is, the larger will be the exciting time. The higher the input current and input power are, the smaller the exciting time will be. In this circuit, the amplitude of the high-frequency current source can be used

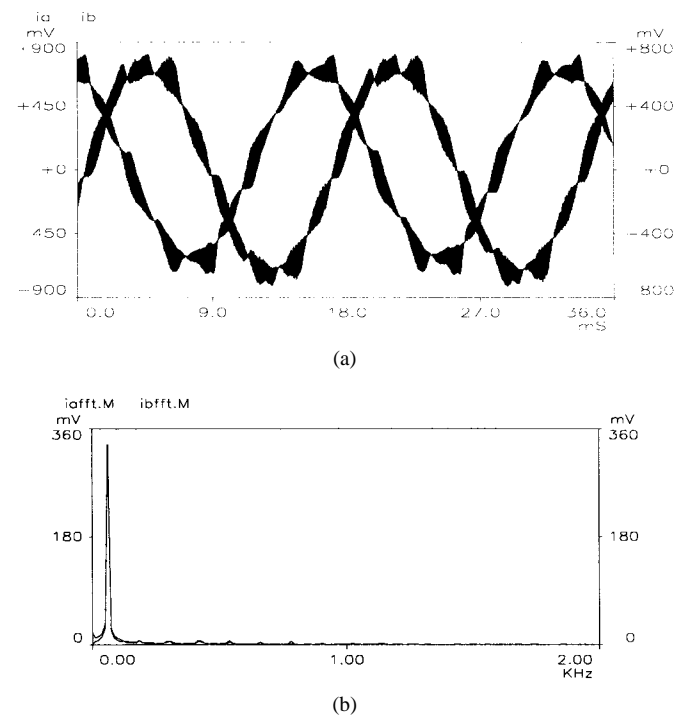


Fig. 10. (a) Experimental waveforms of the input currents. (b) Frequency spectra of the waveforms of Fig. 10(a).

to control the input power. There are several ways to control the amplitude of the current source. The easiest way is to control the switching frequency. An increase in the switching frequency decreases the amplitude of the current source and vice versa.

It is easy to combine three single-phase doubler PFC converters into a three-phase PFC converter as shown in Fig. 7. Since each phase-converter has PFC function, the waveform of each input phase current is almost sinusoidal. For a balanced three-phase system, the sum of the input currents is equal to zero as given by

$$i_a + i_b + i_c = 0. \quad (4)$$

The combination of three single-phase converters shown in Fig. 7 can be simplified as the one shown in Fig. 3. In fact, two single-phase doubler PFC converters can be combined into one single-phase PFC converter as shown in Fig. 8.

From simulation and experiment, it is established that the circuits shown in Figs. 3 and 8 can be used to shape the input current. The THD in the input current can be kept low and the dc output voltage can be chosen very close to the amplitude of the line voltage.

### III. RESULTS

The converter of Fig. 3 was simulated at a line frequency of 600 Hz in order to reduce the simulation time. The waveforms of (600 Hz) input currents are shown in Fig. 9(a). The corresponding frequency spectra are shown in Fig. 9(b), and it is seen that the distortion is very low. The experimental waveforms of the input currents for the three-phase PFC converter of Fig. 3 are shown in Fig. 10(a). Only two of

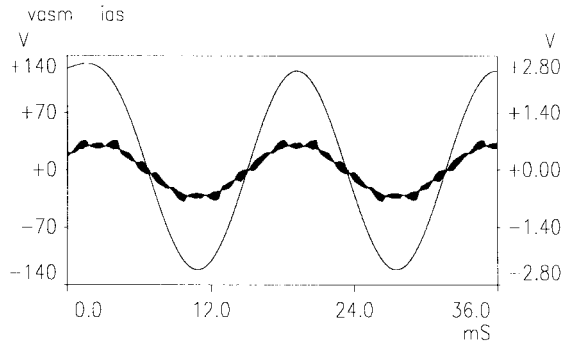


Fig. 11. Waveforms of the input voltage (Phase A) and corresponding current.

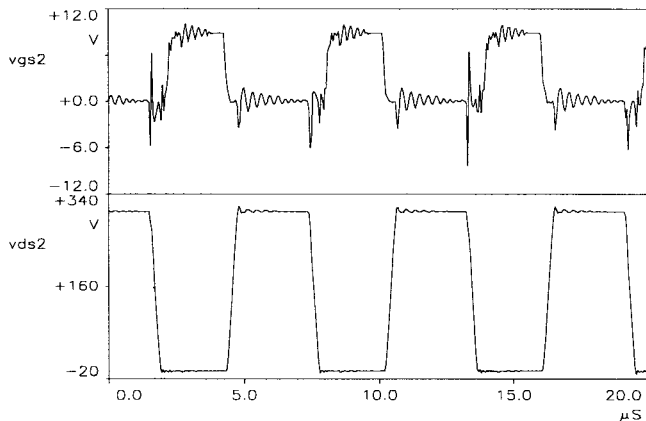


Fig. 12. Waveforms of the gate voltage of  $M_2$  and the drain voltage of  $M_2$ .

the three input currents are shown since only two current probes were available. The frequency spectra of the two input currents are shown in Fig. 10(b) and the THD is measured as 4.5%. The waveforms of the input voltage (Phase A) and the corresponding current are shown in Fig. 11, and it is seen that the two are in phase. The experiment was conducted with an input voltage of 204-V line, rms, and an output dc voltage of 300 V. The switching frequency was selected as 170 kHz. With  $L_a = L_b = L_c = 1.72$  mH,  $C_a = C_b = C_c = 5.1$  nF, and a load resistance of 468  $\Omega$ , the output power is 192 W and the efficiency is 98.0%. The waveforms of the gate voltage of  $M_2$  and the drain voltage of  $M_2$  are shown in Fig. 12. It is seen that there is ZVS for  $M_2$  which is also true for  $M_1$ .

A comparison of the proposed resonant boost input (RBI) PFC converter with the CCM PFC converter and the DCM PFC converter is made and Table I lists the salient features.

As shown in Table I, the RBI PFC converter uses 6 + 2 diodes, which means six ultrafast recovery diodes and two general-purpose diodes. It uses only three boost inductors as compared to six in the case of a DCM PFC. In a power converter, the inductor is an expensive component and also it takes up more space. The inductor also affects the efficiency of the whole system. It is seen that the proposed three-phase PFC converter yields the same or better results (efficiency and THD) as the CCM PFC converter [1], but at a reduced cost by using a fewer switches and a much simpler control circuit. In addition, the proposed circuit is capable of giving an output dc

TABLE I  
COMPARISON OF THREE-PHASE PFC CONVERTERS

Converter type	CCM PFC	DCM PFC	RBI PFC
Features			
No. of switches	6	1	2
No. of diodes	6	7	6+2
No. of inductors (Boost and filter)	3	6	3
No. of capacitors	0	0	3
Ease of loop design	Difficult	Easy	Moderate
Switching condition	Hard-switching	ZCS	ZVS
Voltage gain ( $M$ ) possible	Low	High	Low

voltage much closer to the amplitude of the input line voltage (i.e.,  $M$  is low).

#### IV. CONCLUSIONS

A new topology for a three-phase resonant boost PFC converter is presented. The operation of the converter was explained by identifying the different switching modes for both the resonant input mode and the boost input mode. The simulation and experimental results obtained on a prototype converter were presented. By operating partly under DCM and partly under CCM, the converter has a low input-current THD and a high efficiency. The THD for the experimental converter was measured as 4.5% and the efficiency was 98%.

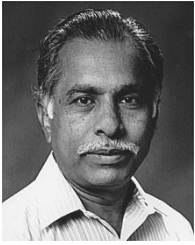
#### REFERENCES

- [1] H. Mao, D. Boroyevich, A. Ravindra, and F. Lee, "Analysis and design of a high frequency three-phase boost rectifier," in *IEEE APEC'96 Rec.*, pp. 538–544.
- [2] A. R. Prasad, P. D. Ziogas, and S. Manias, "An active power factor correction technique for three phase diode rectifiers," in *IEEE PESC'89 Rec.*, pp. 58–66.
- [3] D. F. Weng and S. Yuvarajan, "Constant-switching-frequency ac-dc converter using second-harmonic-injected PWM," in *IEEE APEC'95 Rec.*, pp. 642–646.
- [4] R. Zhang and F. C. Lee, "Optimum PWM pattern for a three-phase boost DCM PFC rectifier," in *IEEE APEC'97 Rec.*, pp. 895–901.
- [5] S. Gataric, D. Boroyevich, and F. C. Lee, "Soft-switched single-switch three-phase rectifier with power factor correction," in *IEEE APEC'94 Rec.*, pp. 738–744.
- [6] C. S. Moo, Y. C. Chuang, and C. R. Lee, "A new power factor correction circuit for electronic ballasts with series-load resonant inverter," in *IEEE APEC'96 Rec.*, pp. 628–633.



**Da Feng Weng** (M'95) received the B.S. and M.E. degrees in electrical engineering from Zhejiang University, Hangzhou, China, in 1982 and 1985, respectively, and the Ph.D. degree in electrical engineering from North Dakota State University, Fargo, in 1995.

From 1985 to 1991, he was a Lecturer in the Department of Electronics, Hangzhou Institute of Commerce, China. Later, he spent about two years as a Visiting Scholar at the Federal University of Santa Catarina, Brazil. From 1995 to 1996, he was a Design Engineer at MagneTek, Huntington, IN, where he worked on electronic ballasts. He is currently with the Research and Development Division, Matsushita Electric Works, Woburn, MA. His research interests include switching power supplies and electronic ballasts.



**S. Yuvarajan** (SM'84) received the B.E. degree (Honors) in electrical engineering from the Government College of Technology, Madras University, Coimbatore, India, in 1966 and the M.Tech. and Ph.D. degrees from the Indian Institute of Technology, Madras, India, in 1969 and 1981, respectively.

From 1969 to 1974, he was a Lecturer in Electrical Engineering at the P.S.G. College of Technology, Coimbatore. He was with the Department of Electrical Engineering at the Indian Institute of Technology, Madras, from 1974 to 1983. He joined the Department of Electrical Engineering at North Dakota State University, Fargo, in 1983, where he is currently a Professor. His research interests include power converters and power semiconductor devices.